Measurement and Prediction of Adsorption Equilibrium for a $H_2/N_2/CH_4/CO_2$ Mixture

Jiaquan Wu, Li Zhou, Yan Sun, and Wei Su
High Pressure Adsorption Laboratory (State Key Laboratory of Chemical Engineering), School of Chemical Engineering and Technology, Tianjin University, Tianjin 300072, China

Yaping Zhou
Dept. of Chemistry, School of Science, Tianjin University, Tianjin 300072, China

DOI 10.1002/aic.11169
Published online March 27, 2007 in Wiley InterScience (www.interscience.wiley.com).

Adsorption equilibrium data for the pure gases, H_2, N_2, CH_4, CO_2, and a $H_2/N_2/CH_4/CO_2$ mixture on activated carbon JX101 were collected by static and dynamic methods, respectively. The tested range covered temperatures of 283–328 K and pressures up to 30×10^5 Pa. The difference in the adsorption mechanisms between the super- and sub-critical components was considered for both correlation of pure gas adsorption and prediction of multicomponent adsorption equilibrium. The surface heterogeneity, interaction among the adsorbed molecules, and the non-ideal behavior of the adsorbed phase were also accounted for. As a consequence, the pure gas adsorption data were accurately correlated, and the multicomponent adsorption equilibrium was satisfactorily predicted by a proposed model. Applicability of the new model was verified with the present experimental data and with literature values. In all cases, the new model produced better agreement between the predicted data and the experimentally measured data than previous models. This indicates that the new model is probably applicable to predict the adsorption equilibrium of gas mixtures either partially or totally composed of supercritical gases. © 2007 American Institute of Chemical Engineers *AIChE J,* 53: 1178–1191, 2007

Keywords: adsorption equilibrium, multicomponent, measurement, prediction, mechanism

Introduction

Adsorption methods appear to be of increasing importance for gas separation/purification and storage technology. Recently, there has been substantial progress in adsorption science and technology especially with the fast development of novel materials that are applicable for adsorption. Understanding multicomponent adsorption equilibrium is necessary for designing a separation process based on adsorption.[1] There are not any theoretical models available for the gas/solid phase equilibrium, although theoretical models are available for phase equilibrium of fluids. Therefore, the prediction of the adsorption equilibrium for a mixture is urgently needed for the practical process design and this is a hot area of research in chemical engineering. Not only is the theoretical prediction of multicomponent adsorption equilibrium difficult, but their measurements are also hard especially for mixtures composed of three or more components. These measurements require tedious and time-consuming experimental procedures[2] and are further complicated by the numerous adsorptive/adsorbent combinations. In fact, not much experimental data for multicomponent adsorption are available in the literature. The procedure for studying multicomponent adsorption is to set up a model to predict the adsorption based on the adsorption isotherms of pure gases. However, such a model needs to be verified with experimental data. Measurement of the adsorp-

Correspondence concerning this article should be addressed to L. Zhou at zhouli@tju.edu.cn.

Table 1. Experimental Conditions of Multicomponent Adsorption

Run	T (K)	100y (H_2)	100y (N_2)	100y (CH_4)	100y (CO_2)
1a	283	34.18	22.54	24.34	18.94
1b	298	34.18	22.54	24.34	18.94
1c	313	34.18	22.54	24.34	18.94
1d	328	34.18	22.54	24.34	18.94
2	283	54.21	8.53	30.05	7.20
3	298	48.87	21.55	21.87	7.70
4	313	27.49	29.12	22.16	21.23
5	328	33.40	24.48	22.82	19.30

tion equilibria of mixtures composed of three or more components is important for practical and theoretical needs, and the present study was thus carried out.

Prediction models for multicomponent adsorption are available in monographs.[3–6] The models frequently referred to in the literature include: the extended Langmuir equation (EL) or the related LRC (laden ratio correlation) model; the adsorption potential theory model[7]; the IAST (ideal adsorption solution theory) model[8]; the HIAST (heterogeneous ideal adsorption solution theory) model[9]; the MPSD (micropore size distribution) model[10]; the MIAST (multispace ideal adsorption solution theory) model[11]; the real adsorption solution theory model[12]; the spreading-pressure-dependent model[13]; the VSM (vacancy solution model)[14–16]; the 2-d EOS (two-dimensional equation of state) model[17]; and the models based on statistical thermodynamics.[18,19] Each model has had predictive success, but is usually for a specific mixture and adsorbent. Most models usually work well for two component mixtures, but not as well for three component mixtures not to mention mixtures of four and more components. Actually, no experimental data for four-component mixtures were available until now. In addition, most experimental data are obtained at relatively low pressure and for a narrow range or, for just one temperature. Therefore, most models have not been verified over a relatively large range of experimental conditions.

Experimental Data

Pure gas adsorption isotherms

Chemicals and Measurement Method. Pure gases of H_2, N_2, CH_4, CO_2, and their mixtures were used in the experiments. The purity of them was above 99.999%, 99.999%, 99.995%, and 99.99%, respectively. Helium of purity above 99.999% was used for the carrier gas. To guarantee uniformity of mixing, enough time was allowed for diffusion and the cylinder containing the mixture was occasionally rolled until the composition reported by GC analysis was unchanged. Activated carbon JX101 was made from coconut shells by Tangshan Activated Carbon Company, China. The sample has a surface area of 1500 m^2/g and the micropore volume was 0.5 cm^3/g, which was determined from CO_2 adsorption at 273 K. Carbon samples were ground to particle sizes of 0.35–0.45 mm and dried to a constant weight under vacuum at 393 K before the experiment.

For each pure component, adsorption isotherms were collected in the temperature range of 283–328 K at 15 K intervals and of pressures up to 30×10^5 Pa in a volumetric setup, which has been described previously.[20]

Collected Adsorption Data. The collected adsorption data for the pure gases on activated carbon JX101 are listed in Appendix A1–A4 for 283, 298, 313, and 328 K and at pressures from 0–30×10^5 Pa.

Four-component mixture adsorption isotherms

Test Conditions and Measurement Method. The experimental conditions for multicomponent adsorption are given in Table 1. Adsorption equilibrium data of the four-component mixture at the aforementioned temperatures and pressures were collected with a dynamic method. The apparatus used is schematically shown in Figure 1. Details of the apparatus and the calculation of the adsorbed amount were previously presented.[21,22] The adsorbed amount determined by a dynamic method is reliable only for the following conditions:[4] The experiments must be isothermal, no pressure drop over the adsorption bed, gas mixture is diluted enough, plug flow, and the equilibrium at the gas/solid interface is instantly achieved. Although the validity of the dynamic method has been previously proven,[22] verification was also carried out in the present study, since the present adsorption pressures were considerably higher than in the previous study. As shown in Figure 2, the pressure and temperature were almost constant during the experiment, and the other conditions were also satisfied.[23] To test the reliability of the dynamic method under the present experimental conditions, a comparison of the adsorbed amounts obtained from static and dynamic methods at the same conditions was made. The results are shown in Figure 3 and there is good agreement between them.

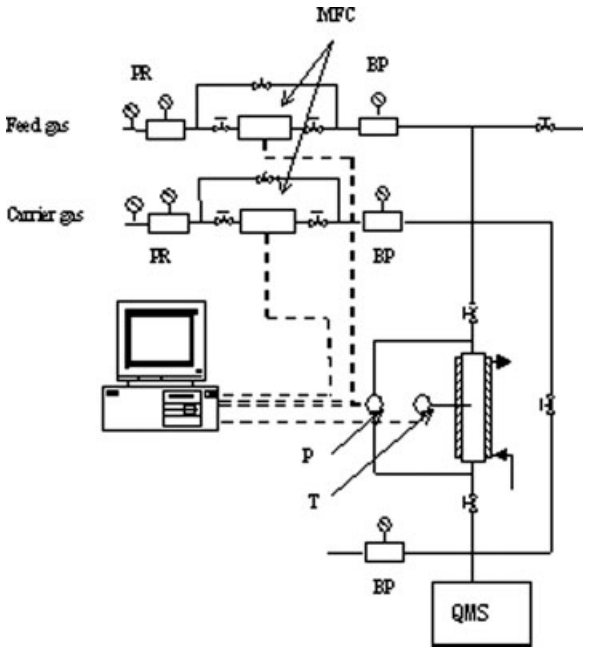

Figure 1. Dynamic method of adsorption measurement.

PR, Pressure regulator; MFC, Mass flow controller; BP, Back pressure regulator; P, Pressure transducer; T, T-type thermocouple; QMS, Quadrapole Mass Spectrometer.

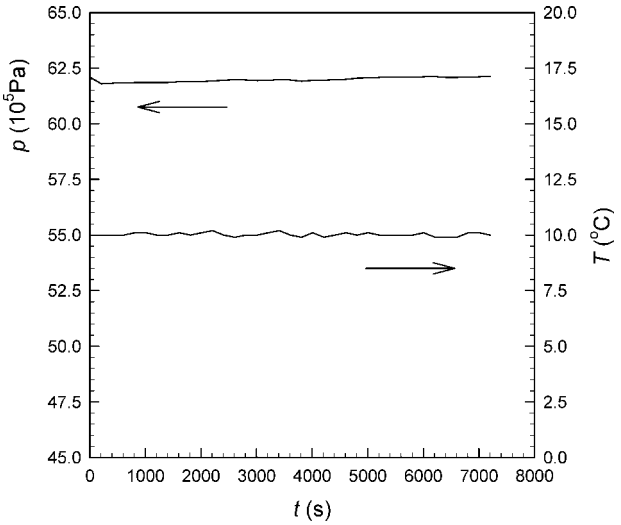

Figure 2. Temperature and pressure detected at the bed center during experiments.

Collected Adsorption Data. The mixture adsorption data are presented in Appendix B1–B8, where the pressure is the sum of the partial pressures of the components.

Correlation of Pure Gas Data and Prediction of Multicomponent Adsorption

Description of adsorbed phase

The adsorption mechanisms of gases on porous solids are different at temperatures below or above the critical temperature.[24–26] Condensation may occur below the critical temperature. Therefore, the adsorbed phase appears to be in a liquid like state, and depending on the structural features of the adsorbents, the adsorption mechanism might be multilayer, volume-filling, or capillary condensation. However, condensation of fluids does not occur above the critical temperature; therefore, adsorption mechanisms originating from condensation do not function above the critical temperature. Multilateral proofs support the claim that only monolayer coverage on solid surfaces occurs at above-critical temperatures.[27–32] Setting up a prediction model for multicomponent adsorption requires that the difference in the adsorption mechanisms be taken into account because quite often there are supercritical components in the mixture especially when the mixture is composed of gases of low molecular weights.

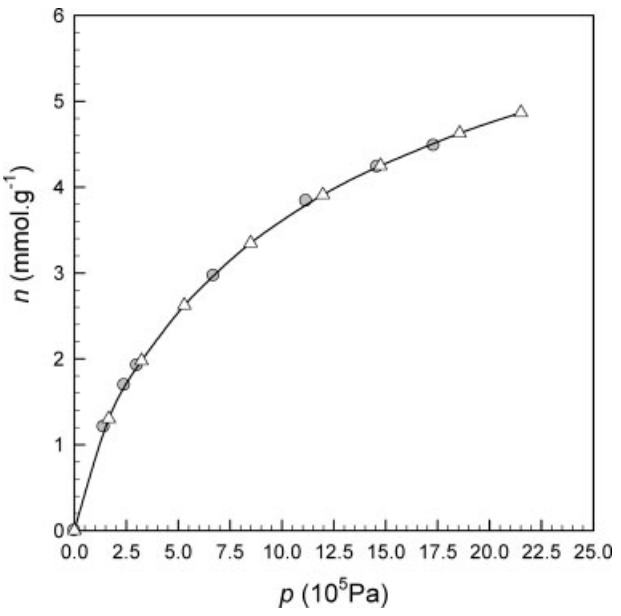

Figure 3. Adsorption isotherm of CH_4 on activated carbon JX101 collected with different methods.

△, By static method; ●, by dynamic method.

The critical properties of the tested gases are listed in Table 2. These together with the experimental conditions given in Table 1 indicate that both subcritical and supercritical gases are present in the $H_2/N_2/CH_4/CO_2$ mixture. Hydrogen, nitrogen, and methane are always supercritical gases at all the conditions tested. However, carbon dioxide is subcritical below 313 K although it changes to supercritical at 328 K. On the basis of the adsorption mechanisms mentioned previously, a simple adsorption picture was drawn for the gas mixture containing both sub- and supercritical components and is shown in Figure 4. In the first layer, any type of molecules (sub- or supercritical) can adsorb. In subsequent layers, molecules can only be adsorbed on top of subcritical molecules. The interaction forces are considerably different for the first layer than for the second and subsequent layers.[27] Therefore, the adsorbed molecules can be divided into two classes: Class I are the first layer adsorbates that adsorb directly on the solid surface; Class II are the second and subsequent layer adsorbates that adsorb on the previously adsorbed molecules as shown in Figure 4.

Model fit criterion

The agreement between a model and the experimental data can be quantified with the average relative difference, which is defined as:

$$\mathrm{ARD} = \frac{1}{N}\sum_{i=1}^{N}\left|\frac{n_{i,\mathrm{exp}} - n_{i,\mathrm{cal}}}{n_{i,\mathrm{exp}}}\right| \times 100 \qquad (1)$$

where N is the total number of data points, $n_{i,\mathrm{exp}}$ is the experimentally measured amount adsorbed and $n_{i,\mathrm{cal}}$ is the amount predicted to be adsorbed by the model. The average relative difference for the amount adsorbed, Δn_i, and the molar fraction of component i in the adsorbed mixture, Δx_i, were calculated from Eq. 1, whereas $\overline{\Delta} n_i$ and $\overline{\Delta} x_i$ are the overall averages for all the components for the amount adsorbed and for the composition of the adsorbed phase, respectively:

$$\mathrm{OARD} = \frac{1}{m}\sum_{i=1}^{m}\mathrm{ARD} \qquad (2)$$

where m is the number of components.

Table 2. Critical Parameters and Eccentric Factors of Tested Gases

Gas	T_c (K)	p_c/100 (KPa)	ω
H_2	33.2	13	−0.218
N_2	126.2	33.9	0.039
CH_4	190.4	46	0.011
CO_2	304.1	73.8	0.239

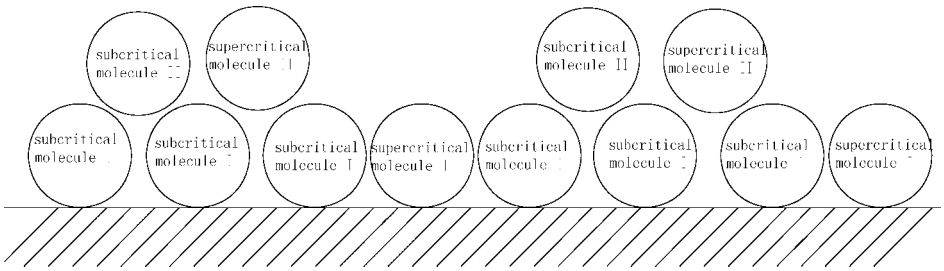

Figure 4. Classification of adsorbed molecules.

Correlation of pure gas adsorption data

The adsorption isotherms of the pure gases provide the values of the parameters used in the model for predicting the adsorption of mixtures. Generally, the total adsorption amount is the sum of the two classes of adsorbates. The surface heterogeneity of adsorbents exerts considerable effect on adsorption, and was accounted for using the PSD (pore size distribution) of the adsorbent.[2,10,33] The total amount adsorbed was calculated for component i using:

$$n_i = \int_{\min,i}^{\infty} (n_{i,\mathrm{I}} + n_{i,\mathrm{II}}) f(r)dr = \int_{\min,i}^{\infty} (n^0_{i,\mathrm{I}}\theta_{i,\mathrm{I}} + n^0_{i,\mathrm{II}}\theta_{i,\mathrm{I}}\theta_{i,\mathrm{II}}) f(r)dr \quad (3)$$

where n_i is the amount adsorbed; the saturated amounts adsorbed of the two classes of adsorbates are given by $n^0_{i,\mathrm{I}}$ and $n^0_{i,\mathrm{II}}$ (i =1, 2, 3, 4); θ_{I} is the fractional surface coverage by class I molecules and θ_{II} is the fractional surface coverage by class II molecules. θ_{II} is proportional to θ_{I} since class II molecules are adsorbed above class I molecules. It is, therefore, assumed that

$$n_{i,\mathrm{II}} = n^0_{i,\mathrm{II}}\theta_{i,\mathrm{I}}\theta_{i,\mathrm{II}}$$

$f(r)$ in Eq. 3 is the PSD function and is assumed to follow the Gamma distribution:

$$f(r) = \frac{q^{v+1}r^v \exp(-qr)}{\Gamma(1+v)} \quad (4)$$

where r equals the half width of the pores; $r_{i,\min}$ is the minimal pore size accessible for component i and is taken as $0.858\sigma_{si}$.[34]

Local Isotherm for Class I Adsorbates. Although the modified Langmuir equation was used in a previous study,[21] considering the much higher adsorption pressures the vacancy solution theory model, FHVSM,[16] was applied here. The FHVSM model accounts for the nonideality of the adsorbed phase by introducing activity coefficients, therefore, is more appropriate than the Langmuir isotherm. The adsorption equilibrium of pure gases is expressed as:

$$p = \left(\frac{n^0_{i,\mathrm{I}}}{b_i}\frac{\theta_{i,\mathrm{I}}}{1-\theta_{i,\mathrm{I}}}\right)\exp\left(\frac{a^2_{iv}\theta_{i,\mathrm{I}}}{1+a_{iv}\theta_{i,\mathrm{I}}}\right) \quad (5)$$

where b_i is the Henry Law constant, $n^0_{i,\mathrm{I}}$ is the saturation amount adsorbed, and a_{iv} is the coefficient of dual interaction. The effect of surface heterogeneity is accounted for by Henry Law constant,

$$b(i,r) = b_{0,i}\ \exp\left(\frac{E(i,r)}{RT}\right) \quad (6)$$

where $E(i,r)$ is the interaction energy between the adsorbate i and the adsorbent surface, whose value is the negative of the minimum potential function, $\varphi(r,z)$, in a pore of radius r and at a distance z from the surface. $E(i,r)$ is, therefore, a function of pore size and, thus, the FHVSM model is correlated with PSD. Adsorption potential is determined using the 10-4-3 form of the Lennard-Jones function:

$$\varphi(r,z) = \frac{5}{3}\varepsilon^*_{si}\left\{\frac{2}{5}\left[\left(\frac{\sigma_{si}}{r+z}\right)^{10} + \left(\frac{\sigma_{si}}{r+z}\right)^{10}\right] - \left[\left(\frac{\sigma_{si}}{r+z}\right)^{4} + \left(\frac{\sigma_{si}}{r+z}\right)^{4}\right] - \left[\left(\frac{\sigma^4_{si}}{3\Delta(0.61\Delta + r + z)^3}\right) - \left(\frac{\sigma^4_{si}}{3\Delta(0.61\Delta + r - z)^3}\right)\right]\right\} \quad (7)$$

$$\varepsilon^*_{si} = \frac{6}{5}\pi\rho_s\varepsilon_{si}\sigma^2_{si}\Delta \quad (8)$$

where ε^*_{si} is the minimum mutual interaction potential between the adsorbed molecules and the single layer of carbon atoms of the surface, σ_{si} is the collision diameter of an i molecule with carbon atoms, Δ is the interstitial distance between the adjacent basal planes of carbon and is taken as 0.335 nm, ρ_s is the number of carbon atoms per unit volume and is taken as 114 nm^{-3}, and ε_{si} is the interaction potential between a carbon atom and an i molecule. The Lorentz–Berthlot rule is used for the calculation of σ_{si} and ε_{si}:

$$\sigma_{si} = \frac{\sigma_{ss} + \sigma_{ii}}{2} \quad (9)$$

$$\varepsilon_{si} = \sqrt{\varepsilon_{ss} \times \varepsilon_{ii}} \quad (10)$$

Local Isotherm for Class II Adsorbates. The Langmuir adsorption isotherm was used for class II adsorbates because of its simplicity and convenience of use and also due to the fact that the adsorption potential for class II adsorbates is independent of PSD according to the BET theory of adsorption. Therefore, the coefficient of the Langmuir equation, k_{II}, is a constant and the adsorption amount of class II adsorbates is given by

$$n_{\mathrm{II}} = n^0_{\mathrm{II}}\theta_{\mathrm{I}}\theta_{\mathrm{II}} = n^0_{\mathrm{II}}\theta_{\mathrm{I}}\frac{k_{\mathrm{II}}p}{1+k_{\mathrm{II}}p} \quad (11)$$

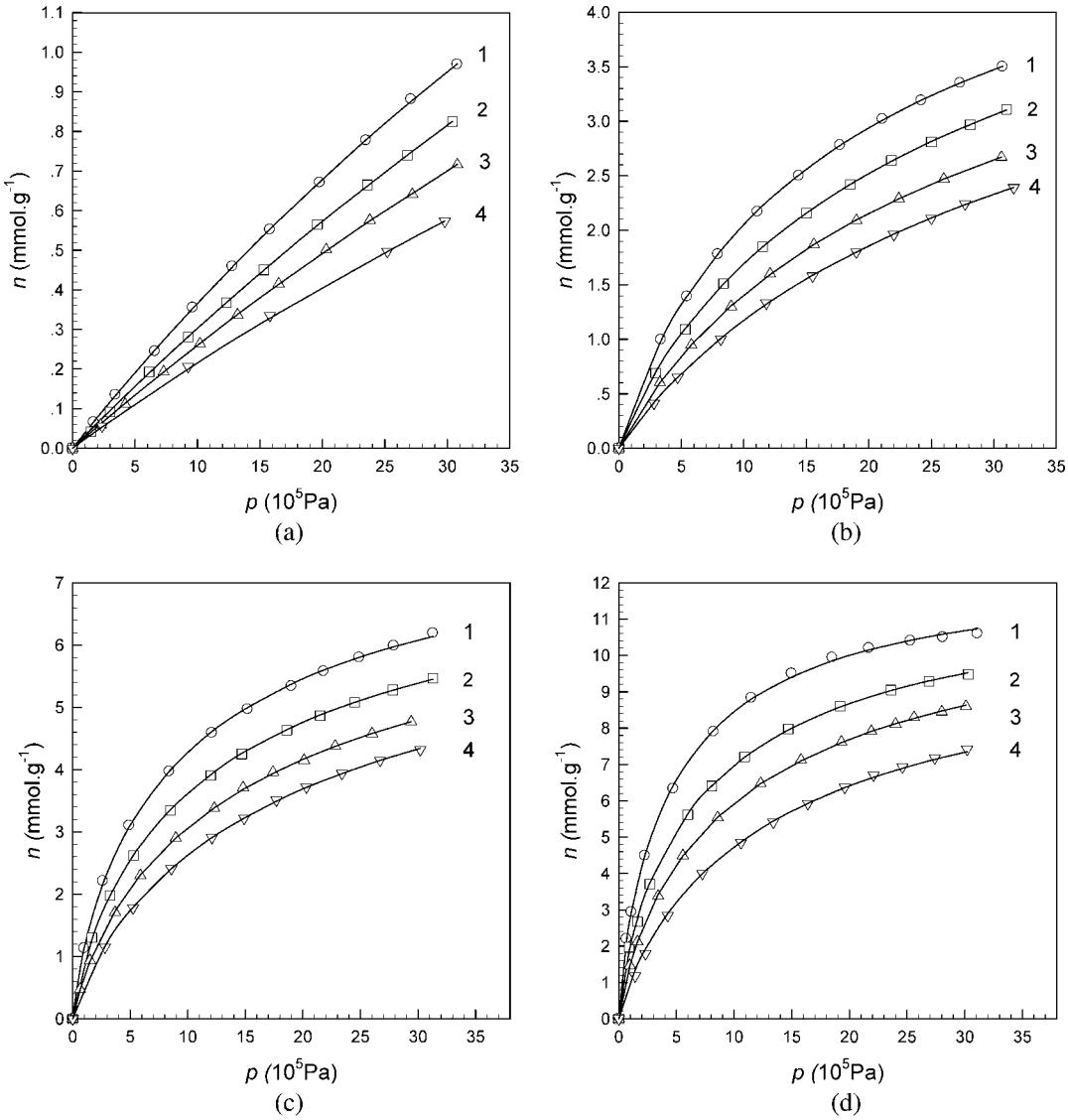

Figure 5. Data and correlation for the adsorption of pure gases on activated carbon JX101. Symbols, experimental data; Curves, model predicted.

(a) H_2 1: 283 K; 2: 298 K; 3: 313 K; 4: 328 K. (b) N_2 1: 283 K; 2: 298 K; 3: 313 K; 4: 328 K. (c) CH_4 1: 283 K; 2: 298 K; 3: 313 K; 4: 328 K. (d) CO_2 1: 283 K; 2: 298 K; 3: 313 K; 4: 328 K.

For the monolayer adsorption mechanism, there are not any class II adsorbates for pure supercritical gases. Therefore, there are only five parameters in the isotherm model: $n^0_{i,\mathrm{I}}$, b_0, a_{iv}, q, and v, where q and v are properties of adsorbents. However, the multilayer adsorption mechanism for subcritical gases adds two more parameters, $n^0_{i,\mathrm{II}}$ and $k_{\mathrm{II},i}$, to the isotherm model. Since parameters q and v describe properties of the adsorbent, they do not change for different gas components.

The fit of the correlation model to the experimental data for the pure gases is shown in Figures 5a–d. The average relative differences are shown in the last row of Table 3, which are less than 2%.

Prediction of multicomponent adsorption

Proposed Model. A new model (ATCANI) was proposed for the prediction of multicomponent adsorption on the basis of admitting two classes of adsorbates and the nonideality of the adsorbed phase. Taking a four-component mixture as an example, the model is expressed as:

$$n_i = \int_{\min,\mathrm{i}}^{\infty} (n_{i,\mathrm{I}}(P,T,y_1,y_2,y_3,y_4) + n_{i,\mathrm{II}}(P,T,y_1,y_2,y_3,y_4))f(r)dr \quad (12)$$

$$n_t = \sum_{i=1}^{4} n_i \quad (13)$$

To account for the nonideality of the adsorbed phase, the activity coefficient was introduced in the model as the FHVSM model usually does.

Table 3. Parameter Values Used in the Prediction Model for Multicomponent Adsorption

Parameter	T(K)	H_2	N_2	CH_4	CO_2
$n^0_{i,\mathrm{I}}$	283	6.4340	6.0925	8.5967	10.9686
	298	6.2452	6.0105	8.1306	10.8829
	313	5.7546	5.7576	7.9138	10.9410
	328	2.8481	5.7450	7.4221	12.4593
$n^0_{i,\mathrm{II}}$	283	1.2188	1.1541	1.6285	2.0778
	298	1.1684	1.1245	1.5211	2.0360
	313	1.1457	1.1463	1.5756	2.1783
	328	0	0	0	0
b_0 ($\times 10^8$ Pa)	283	5.3201	5.7173	4.2631	2.0352
	298	4.7552	5.1332	4.0403	2.0201
	313	4.4647	4.8548	3.9025	1.8985
	328	4.3260	4.4162	3.3773	1.3458
$a_{i,v}$	283	0.6966	0.8385	1.1928	0.4658
	298	0.4576	0.7964	1.1352	0.9482
	313	0.5511	0.8317	1.1677	1.1276
	328	0.3778	0.7990	0.8456	0.2863
k_{II}	283	0.5406	0.5997	0.4540	0.2217
	298	0.5840	0.6507	0.5201	0.2659
	313	1.0940	1.2277	1.0019	0.4985
	328	0	0	0	0
q	283–328		17.89		
v	283–328		92.27		
ARE%	283–328	1.32	0.24	0.51	1.09

$$y_i \Phi_i p = y_i^s x_i \frac{n_{m,\mathrm{I}}}{n^0_{m,\mathrm{I}}} \frac{n^0_{i,\mathrm{I}}}{b(i,r)} \left[\frac{\exp(a_{iv})}{1+a_{iv}}\right] \times \exp\left\{\left[\frac{n^0_{i,\mathrm{I}} - n^0_{m,\mathrm{I}}}{n_{m,\mathrm{I}}} - 1\right] \ln \gamma_v^s x_v^s\right\} \quad (14)$$

$$\ln \gamma_i^s = -\ln \sum_{j=1}^{j=M} \frac{x_j^s}{a_{ij}+1} + \left[1 - \left(\sum_{j=1}^{j=M} \frac{x_j^s}{a_{ij}+1}\right)^{-1}\right] \quad (15)$$

$$a_{ij} = \frac{a_{iv}+1}{a_{jv}+1} - 1 \quad (16)$$

where a_{ij} is the mutual interaction parameter and can be obtained from the parameters of the pure gases, which is one reason the FHVSM model was chosen. However, the nonideality must be less in the adsorbed phase formed by class II adsorbates due to the much weaker interactions among them[27] and, therefore, for simplicity, the EL equation was applied for this class of adsorbates.

Supercritical components can be class II adsorbates if the underneath class I adsorbate is subcritical. The probability for a supercritical component to be a class II adsorbate, named formation factor, $L_{\mathrm{sup,II}}$, is proportional to the probability of subcritical components being class I adsorbates, therefore,

$$L_{\mathrm{sup,II}} = \sum x_{\mathrm{sub,I}} \quad (17)$$

$$L_{\mathrm{sub,II}} = 1 \quad (18)$$

where the subscript "sup" indicates supercritical component, "sub" indicates subcritical component, and x is the molar fraction in the adsorbed mixture. Because of the monolayer adsorption mechanism of supercritical gases, the isotherm model for pure gas adsorption cannot provide the values of parameters $n^0_{\mathrm{sup,II}}$ and $k_{\mathrm{sup,II}}$, which are, however, needed by the prediction model for multicomponent adsorption. Therefore, an estimation was made according to the following assumption: If the ratio of saturated adsorption capacities for the two classes of supercritical adsorbates is close to that of the subcritical adsorbates, then the saturation parameter of the supercritical components, $n^0_{\mathrm{sup,II}}$, can be numerically estimated on the basis of the average ratio of subcritical components:

$$\frac{n^0_{\mathrm{sup,I}}}{n^0_{\mathrm{sup,II}}} = \frac{1}{h}\sum_{i=1}^{h} \frac{n^0_{\mathrm{sub},i,\mathrm{I}}}{n^0_{\mathrm{sub},i,\mathrm{II}}} \quad (19)$$

where h is the number of subcritical components in the mixture. Another assumption was made about the ratio of adsorption potentials in between adsorbates and that between the adsorbates and the solid surface. It was assumed that these ratios are nearly equal for all components in the mixture, so that the ratio of parameters that reflect the adsorption potentials is nearly equal for all components. The potential parameter was evaluated for class I adsorbates from the FHVSM model, and for class II adsorbates from the Langmuir coefficient to give:

$$\frac{\mathrm{k}_{\mathrm{sup,I}}}{\mathrm{k}_{\mathrm{sup,II}}} = \left(\prod_{i=1}^{h} \frac{k_{\mathrm{sub},i,\mathrm{I}}}{k_{\mathrm{sub},i,\mathrm{II}}}\right)^{\frac{1}{h}} \quad (20)$$

The amount adsorbed of class II adsorbates is then calculated from:

$$n_{i,\mathrm{II}} = n^0_{i,\mathrm{II}} \theta_{\mathrm{I}} L_{i,\mathrm{II}} \frac{k_{i,\mathrm{II}} p_i}{1 + \sum_{i=1}^{m} k_{i,\mathrm{II}} p_i} \quad (21)$$

For this study, $m = 4$. All the parameters needed to predict the adsorption equilibrium of a mixture were available, and the prediction was carried out on the basis of Eq. 12. Because the adsorption pressure is relatively high, the pressure quantity in the equation was replaced by fugacity, which is evaluated via the SRK equation of state.[35] For pure gas:

$$\ln\frac{f}{P} = Z - 1 - \ln(Z - B^*) - \frac{A^*}{B^*}\ln\left(1 + \frac{B^*}{Z}\right) \quad (22)$$

The compressibility factor is determined by the equation

$$Z^3 - Z^2 + Z(A^* - B^* - B^{*2}) - A^*B^* = 0 \quad (23)$$

where

$$A^* = \frac{aP}{R^2T^2} \quad (24)$$

$$B^* = \frac{bP}{RT} \quad (25)$$

$$a = 0.42748\alpha\frac{R^2T_{\mathrm{c}}^2}{P_{\mathrm{c}}} \quad (26)$$

$$b = 0.08664\frac{RT_{\mathrm{c}}}{P_{\mathrm{c}}} \quad (27)$$

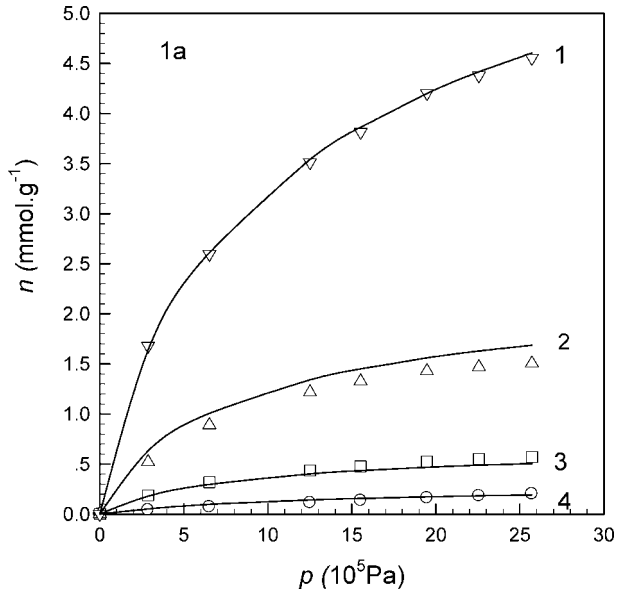

Figure 6. Data and correlation for the adsorption isotherms of the mixture for Run 1a.

Symbols, experimental; curves, model predicted.

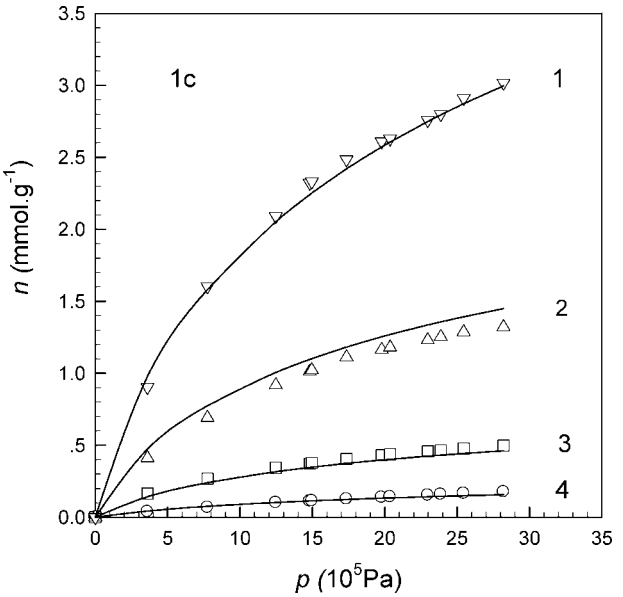

Figure 8. Data and correlation for the adsorption isotherms of the mixture for Run 1c.

Symbols, experimental; curves, model predicted.

$$\alpha^{0.5} = 1 + m(1 - T_r^{0.5}) \tag{28}$$

$$m = 0.480 + 1.574\omega - 0.176\omega^2 \tag{29}$$

For gas mixture:

$$\ln\frac{f_i}{Py_i} = \frac{b_i}{b}(Z-1) - \ln(Z-B^*) - \frac{A^*}{B^*}\left(2\frac{a_i^{0.5}}{a^{0.5}} - \frac{b_i}{b}\right)\ln\left(1+\frac{B^*}{Z}\right) \tag{30}$$

The mixing rule:

$$a = \left(\sum_{i=1}^{c} y_i a_i^{0.5}\right)^2 \tag{31}$$

$$b = \sum_{i=1}^{c} y_i b_i \tag{32}$$

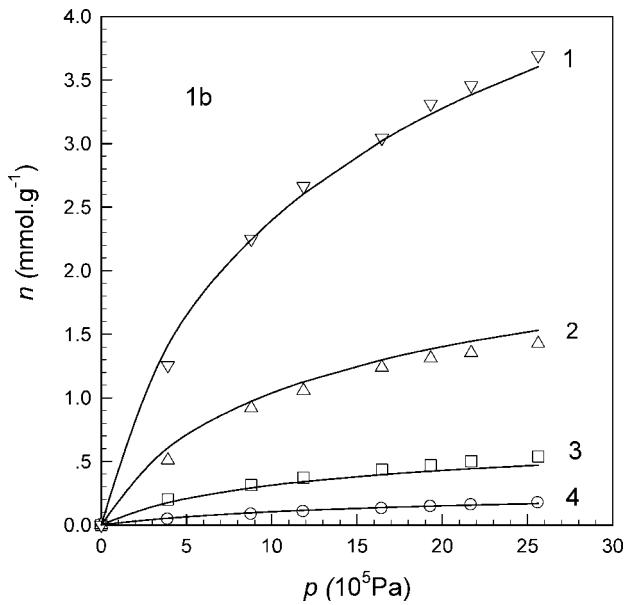

Figure 7. Data and correlation for the adsorption isotherms of the mixture for Run 1b.

Symbols, experimental; curves, model predicted.

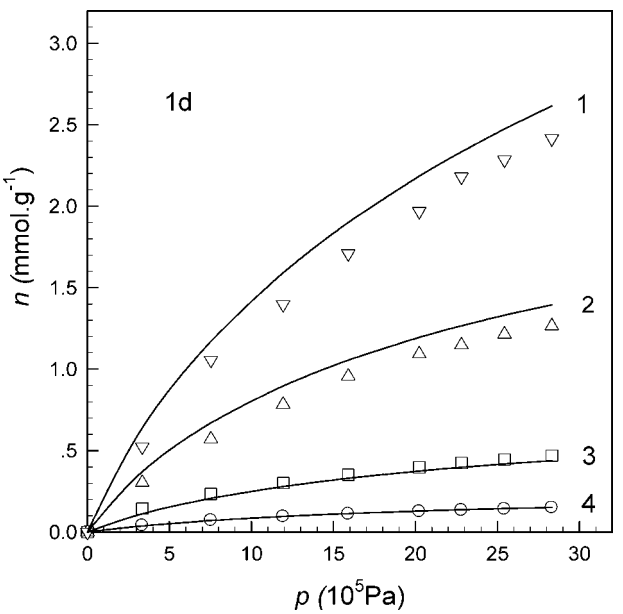

Figure 9. Data and correlation for the adsorption isotherms of the mixture for Run 1d.

Symbols, experimental; curves, model predicted.

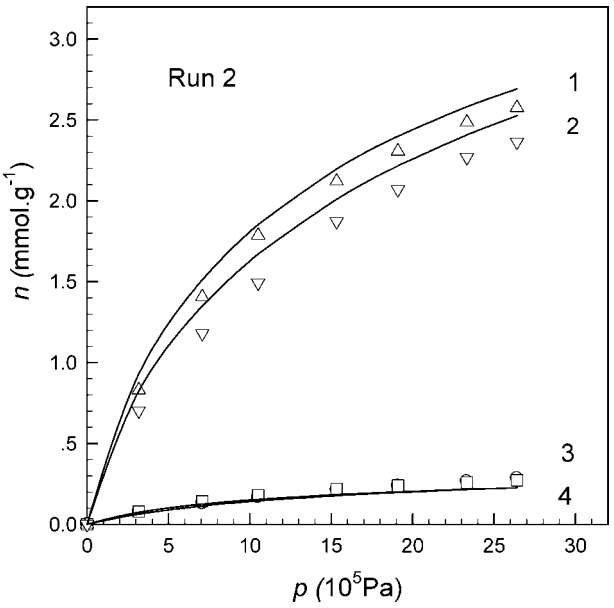

Figure 10. Data and correlation for the adsorption isotherms of the mixture for Run 2.

Symbols, experimental; curves, model predicted.

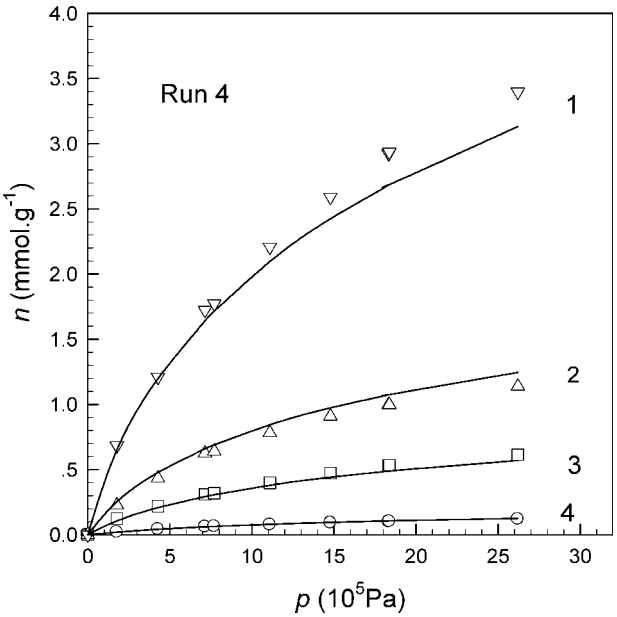

Figure 12. Data and correlation for the adsorption isotherms of the mixture for Run 4.

Symbols, experimental; curves, model predicted.

Verification of the model. Applicability of the constructed model was verified with the experimental data obtained from the present study, our previous studies[21,22] and that published in the literature.[36,37] Parameter values used in the prediction model were evaluated from the adsorption isotherms of the pure gases and are listed in Table 3.

Verification with the present experimental data. The fit of the prediction model with the present experimental data for multicomponent adsorption is shown in Figures 6–13 and the average difference between the model and the experimental data is summarized in Table 4 for different conditions. As shown in Table 4, the overall average of the relative difference is about 10% for both component adsorption, $\overline{\Delta}n_i$, and composition of the adsorbed phase, $\overline{\Delta}x_i$.

To compare the proposed model with the models available in the literature, the present experimental data were used for the EL model, the MREL (Multi-Region Extended Langmuir) model,[38] the LRC model, the IAST model, the FHVSM

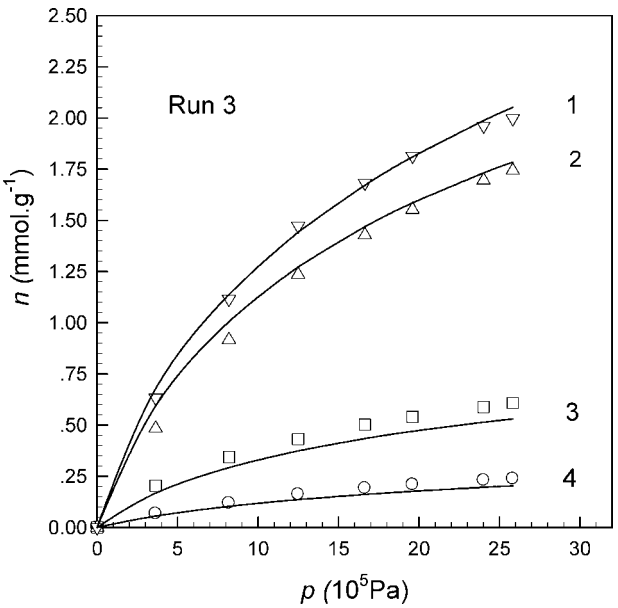

Figure 11. Data and correlation for the adsorption isotherms of the mixture for Run 3.

Symbols, experimental; curves, model predicted.

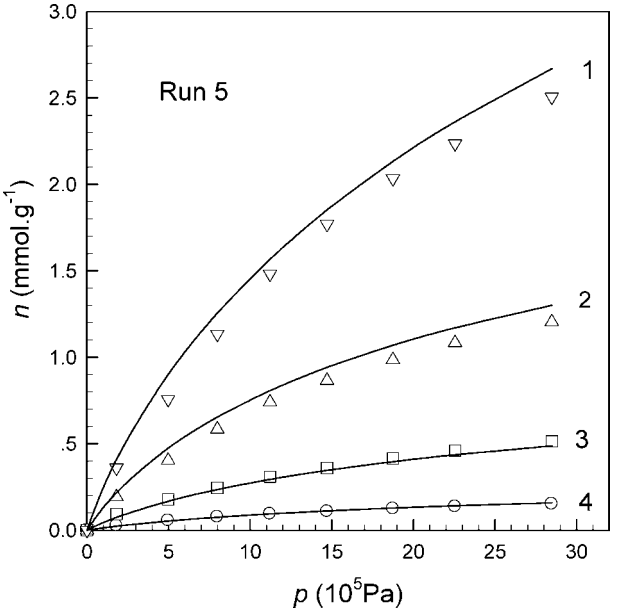

Figure 13. Data and correlation for the adsorption isotherms of the mixture for Run 5.

Symbols, experimental; curves, model predicted.

Table 4. Prediction Error of the Proposed Model for the Present 4-Component Adsorption

Runs	Δn_{H_2} (%)	Δn_{N_2} (%)	Δn_{CH_4} (%)	Δn_{CO_2} (%)	$\overline{\Delta} n_i$ (%)	$\overline{\Delta} x_i$ (%)
1a	16.50	8.76	12.31	1.02	9.65	9.3
1b	9.31	10.33	7.99	3.25	7.72	6.6
1c	6.30	8.28	9.04	2.16	6.45	5.9
1d	2.60	9.02	12.94	11.61	9.04	7.5
2	16.23	13.72	5.59	10.12	11.42	11.0
3	15.46	14.04	6.41	2.30	9.55	9.3
4	3.41	7.22	8.41	5.55	6.15	6.2
5	4.35	6.89	10.63	8.84	7.68	6.3

model, the MPSD model, and the MISC model.[21] Discrepancies between these models and the present experimental data for predicting the component adsorption and the composition of the adsorbed phase are shown in Figures 14 and 15, respectively. Our proposed model is remarkably better than the others and the IAST model is the worst indicating a large degree of nonideality of the adsorbed phase. Our present ATCANI model is a considerable improvement over our previous MISC model. This is largely due to the modification of the local isotherm and accounting for the nonideality of the adsorbed phase. A modified Langmuir equation was used as the local isotherm in the MISC model; however, it is not appropriate to neglect the mutual interactions of the adsorbates at high-pressure conditions. In addition, IAST was used for the mixture adsorption in MISC, which is not appropriate for an adsorbed phase with strong nonideality.

Verification with the data of Reich et al.[36]. Reich et al. measured the adsorption of a $CH_4 + C_2H_4 + C_2H_6$ mixture on BPL activated carbon at 301 K and for pressures up to 30×10^5 Pa. A comparison is made between the proposed model and the LRC and IAST models. The results of the comparison are shown in Table 5. Remarkable improvement is achieved with the proposed model for this set of data.

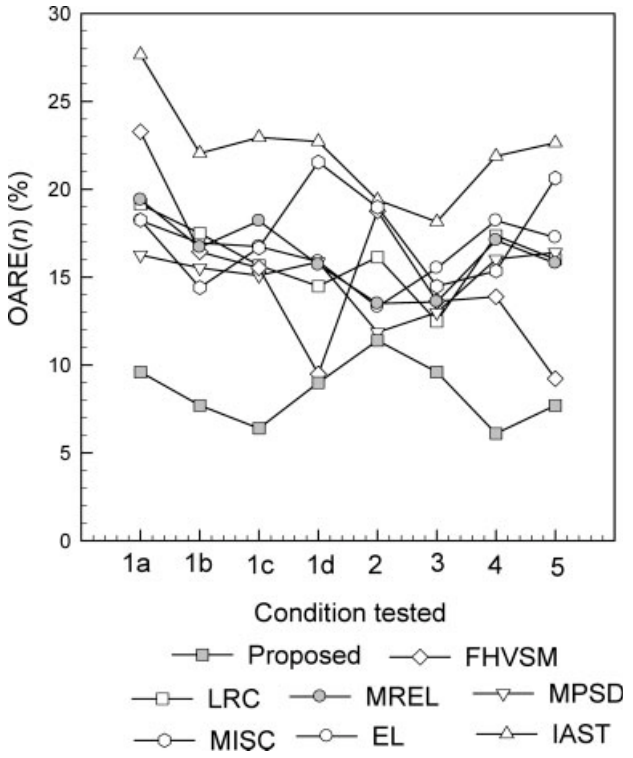

Figure 14. A comparison of models in predicting component adsorption.

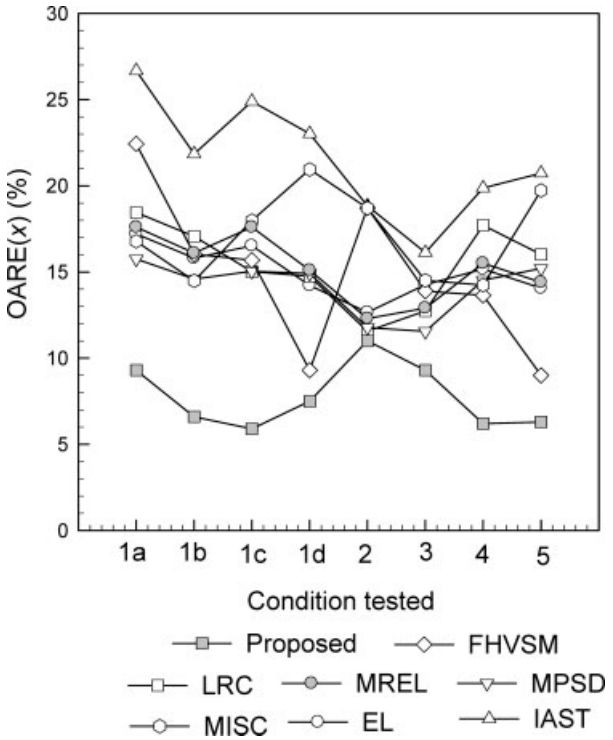

Figure 15. A comparison of models in predicting the composition of the adsorbed phase.

Verification with the data of Dreisbach et al[37]. Dreisbach et al. measured the adsorption of a CH_4+CO_2+N_2 mixture on activated carbon NoriR1 at 298 K and presented a GDSL (Generalized Dual-Site Langmuir) model. This set of data was applied to the proposed model and the results of comparison are shown in Table 6. Remarkable improvement is again observed with the proposed model for this set of data.

Verification with our previous data. Adsorption data of a CH_4+CO_2+C_2H_6 mixture on activated carbon JX101 were measured at different temperature and pressures using the

Table 5. Comparison of the Proposed Model with IAST and LRC Using the Data of Reich et al.

	LRC	IAST	Proposed
Δn_1	39.44	50.94	17.61
Δn_2	17.79	7.23	6.54
Δn_3	19.03	11.17	9.40
$\overline{\Delta} n_i$	25.48	23.11	11.18
Δn_t	7.86	6.52	3.25
Δx_1	33.16	43.96	16.27
Δx_2	16.81	9.68	5.31
Δx_3	18.50	9.13	10.59
$\overline{\Delta} x_i$	22.82	20.92	10.72

Component 1, 2, and 3 denote CH_4, C_2H_4, and C_2H_6, respectively.
Values are given in percentage.

Table 6. Comparison of the Proposed Model with LRC, IAST, and GDSL Using the Data of Dreisbach et al.

	LRC	IAST	GDSL	Proposed
Δn_1	25.07	25.86	14.20	7.31
Δn_2	22.14	29.18	9.757	4.86
Δn_3	37.91	49.11	37.97	15.74
$\overline{\Delta n_i}$	28.37	34.72	20.64	9.30
Δn_t	20.00	7.425	4.880	4.00
Δx_1	6.401	15.64	10.79	4.97
Δx_2	14.15	30.05	15.11	1.49
Δx_3	28.02	48.06	35.53	18.49
$\overline{\Delta x_i}$	16.19	32.92	20.48	8.32

Component 1, 2, and 3 denote CH_4, CO_2, and N_2, respectively.
Values are given in percentage.

Table 8. Comparison of the Proposed Model with EL, LRC, MPSD, and SAEM Using Data from Ref. 22

	EL	LRC	MPSD	SAEM	Proposed
Δn_1	42.38	46.13	39.70	38.68	37.41
Δn_2	7.29	7.92	6.25	9.66	6.68
Δn_3	14.70	10.22	9.96	5.06	6.12
$\overline{\Delta n_i}$	13.77	10.95	10.60	7.63	7.11
Δn_t	31.85	39.30	32.08	33.48	32.40
Δx_1	13.08	11.13	7.92	3.61	8.08
Δx_2	1.39	1.82	1.34	2.80	1.49
Δx_3	21.43	21.40	18.63	17.78	16.74
$\overline{\Delta x_i}$	15.43	17.43	13.78	13.28	13.99

Component 1, 2, and 3 denote H_2, N_2, and CH_4, respectively.
Values are given in percentage.

same experimental setup.[21] Taking the data for 298 K as an example, the validity of the present model is verified and a comparison with other models is shown in Table 7. For this set of data, although the present model is not much better than the MISC model, it is considerably better than the other models.

The experimental data above used are for the adsorption of mixtures that contain both super- and subcritical components. In these mixtures, the adsorbed phase deviates greatly from ideality and the proposed model works best for those conditions. Another of our previous works deals with the adsorption of CH_4+N_2+H_2 mixtures that contain only supercritical components.[22] A prediction model, SAEM, was presented for this kind of mixture. Performance of the proposed model for this set of data was verified and comparison was made with other models. The results are shown in Table 8. For this data set, the proposed model works as well as the SAEM model, and it is better than other models.

Conclusions

(1) Adsorption data of a CO_2+CH_4+N_2+H_2 mixture on activated carbon was measured by a dynamic method in the temperature range 283–328 K and at pressures up to 3 MPa. This set of data provides a good basis of verifying prediction models for multicomponent adsorption because the measurements covered a relatively large range of temperature and pressure conditions and the mixture contains both super- and subcritical components. In addition, the adsorbed phase shows a large degree of nonideality.

(2) A new model, ATCANI, to predict multicomponent adsorption is proposed. The new model divides the adsorbed adsorbates into two classes based on the difference of adsorption mechanisms on crossing the critical temperature. The FHVSM model and the Langmuir model were used as the local isotherms for the two classes of adsorbates. As such, the different adsorption mechanisms and the nonideality of the adsorbed phase are accounted for. The effect of the surface heterogeneity of the adsorbent was also accounted for with the PSD function and the Lennard-Jones potential function applied to each pore.

(3) The validity of the proposed model was verified not only with the presently measured data, but also with previous experimental data. The proposed model works better than the other available models for all data tested. It works well for mixtures of different compositions and for adsorbed phases with different degrees of nonideality.

Table 7. Comparison of the Proposed Model with EL, IAST, FHVSM, MPSD, and MISC Using Data from Ref. 21

	EL	IAST	FHVSM	MPSD	MISC	Proposed
Δn_1	29.14	33.18	35.92	32.75	9	9.15
Δn_2	11.48	11.83	27.93	17.64	12.7	7.55
Δn_3	21.01	22.05	23.45	17.92	6.11	6.61
$\overline{\Delta n_i}$	20.54	22.35	29.1	22.77	9.3	7.77
Δn_t	14.33	13.92	14.71	14.17	7.33	4.57
Δx_1	38.94	40.26	57.72	40.23	8.56	7.34
Δx_2	18.11	28.44	30.54	17.25	6.3	7.62
Δx_3	10.84	10.75	18.24	12.08	1.46	4.10
$\overline{\Delta x_i}$	22.63	26.48	35.5	23.19	5.44	6.35

Component 1, 2, and 3 denote CH_4, CO_2, and C_2H_6, respectively.
Values are given in percentage.

Acknowledgments

The financial support of the National Natural Science Foundation of China (grant number 20336020) and that from the Special Funds of Major State Basic Research Projects (2006CB705807) is greatly appreciated.

Notation

a = parameter of the FHVSM model
ARD = average relative difference, %
b_0 = prepotential coefficient, $\times 10^8$ Pa^{-1}
f = fugacity, 10^5 Pa
E = adsorption potential, kJ/mol
h = number of subcritical components
k = coefficient in Langmuir equation
L = formation factor
m = number of components in mixture
n = amount adsorbed, mmol/g
P = pressure, 10^5 Pa
r = pore radius
R = gas constant, J/mol/K
T = temperature, K
x = molar fraction of component in adsorbed phase
y = molar fraction of component in gas phase
z = distance between adsorbate molecule and solid surface, nm
Z = compressibility factor

Greek letters

ω = eccentric factor
Φ = fugacity cvvoefficient
γ = activity coefficient
ε = interaction potential between adsorbate molecules, kJ/mol

φ = potential function, kJ/mol
σ = collision diameter of molecules, nm
θ = fractional surface coverage

Superscript

0 = saturation

Subscripts

c = critical
i = component
s = carbon atoms
I = class I
II = class II
sup = supercritical
sub = subcritical

Literature Cited

1. Qiao SZ, Wang K, Hu XJ. Using local IAST with micropore size distribution to predict multicomponent adsorption equilibrium of gases in activated carbon. *Langmuir*. 2000;16:1292–1298.
2. Hu XJ. Multicomponent adsorption equilibrium of gases in zeolite: effect of pore size distribution. *Chem Eng Commun*. 1999;174:201–214.
3. Ruthven DM. *Principles of Adsorption and Adsorption Processes*. New York: Wiley, 1984.
4. Yang RT. *Gas Separation by Adsorption Processes*. Boston: Butterworths, 1987.
5. Do DD. *Adsorption Analysis: Equilibria and Kinetics*, London: Imperial College Press, 1998.
6. Schwarz JA, Contescu CL. *Surfaces of Nanoparticles and Porous Materials*, New York: Marcel Dekker, 1999:392.
7. Grant RJ, Manes M. Adsorption of binary hydrocarbon gas mixtures on activated carbon. *Ind Eng Chem Fundam*. 1966;5:490–498.
8. Myers AL, Prausnitz JM. Thermodynamics of mixed-gas adsorption. *AIChE J*. 1965;11:121–127.
9. Valenzuela DP, Myers AL, Talu O, Zwiebel I. Adsorption of gas mixtures: effect of energetic heterogeneity. *AIChE J*. 1988;34:397–402.
10. Hu XJ, Do DD. Effect of pore size distribution on the prediction of multicomponent adsorption equilibria. In: LeVan MD, editor. *Fundamentals of Adsorption,* 5th ed. Boston: Kluwer Academic, 1996: 385–392.
11. Eiden U, Schlünder EU. Adsorption equilibria of pure vapors and their binary mixtures on activated carbon. *Chem Eng Process*. 1990; 28:1–22.
12. Costa E, Sotelo JL, Calleja G, Marron C. Adsorption of binary and ternary hydrocarbon gas mixtures on activated carbon: experimental determination and theoretical prediction of the ternary equilibrium data. *AIChE J*. 1981;27:5–12.
13. Talu O, Zweibel I. Multicomponent adsorption equilibria of nonideal mixtures. *AIChE J*. 1986;32:1263–1276.
14. Suwanayuen S, Danner RP. A gas adsorption isotherm equation based on vacancy solution theory. *AIChE J*. 1980;26:68–76.
15. Suwanayuen S, Danner RP. Vacancy solution theory of adsorption from gas mixtures. *AIChE J*. 1980;26:76–82.
16. Cochran TW, Kabel RL, Danner RP. The vacancy solution model of adsorption-improvements and recommendations. *AIChE J*. 1985;31: 2075–2082.
17. Zhou CH, Hall F, Gasem KAM, Robinson RL. Predicting gas adsorption using two-dimensional equations of state. *Ind Eng Chem Res*. 1994;33:1280–1289.
18. Ruthven DM, Loughlin KF, Holborow KA. Multicomponent sorption equilibrium in molecular sieve zeolites. *Chem Eng Sci*. 1973;28: 701–710.
19. Ruthven DM, Wong F. Generalized statistical model for the prediction of binary adsorption equilibria in zeolites. *Am Chem Soc*. 1985; 24:27–32.
20. Zhou YP, Zhou L. Experimental study on high-pressure adsorption of hydrogen on activated carbon. *Sci China (Ser B)*. 1996;39:598–607.
21. Zhou L, Wu JQ, Li M, Wu Q, Zhou YP. Prediction of multicomponent adsorption equilibrium of gas mixtures including supercritical components. *Chem Eng Sci*. 2005;60:2833–2844.
22. Wu Q, Zhou L, Zhou YP, Wu JQ. Prediction of the adsorption equilibrium of mixtures composed of supercritical gases. *J Colloid Interface Sci*. 2004;276:277–283.
23. Wu, JQ. Studies on multicomponent adsorption equilibrium of gas mixture on porous solids. Doctoral Thesis, School of Chemical Engineering and Technology, Tianjin University, Tianjin, China, 2006.
24. Zhou L, Bai SP, Su W, Yang J, Zhou YP. Comparative study of the excess versus absolute adsorption of CO_2 on superactivated carbon for the near-critical region. *Langmuir*. 2003;19:2683–2690.
25. Findenegg GH. High pressure physical adsorption of gases on homogeneous surface. In: Belfort G, Myers AL. eds. *Fundamental of Adsorption*, Schlos Elmau: Bavaria, West Germany, 1983:207–218.
26. Zhou L, Zhou YP, Li M, Chen P, Wang Y. Experimental and modeling study of the adsorption of supercritical methane on a high surface carbon. *Langmuir*. 2000;16:5955–5959.
27. Beebe BA, Biscoe J, Smith WR, Wendell CB. Heats of adsorption on carbon black. I. *J Am Chem Soc*. 1947;69:95–101.
28. Schneider MS, Grunwaldt JD, Baiker A. Near-critical CO_2 in mesoporous silica studied by in situ FTIR spectroscopy. *Langmuir*. 2004;20:2890–2899.
29. Ströbel R, Jörisen L, Schliermann T, Trapp V, Schütz W, Bohmhammel K, Wolf G. Garche J. Hydrogen adsorption on carbon materials. *J Power Source*. 1999;84:221–224.
30. Nijkamp MG, Raaymakers JEMJ, van Dillen AJ, de Jong KP. Hydrogen storage using physisorption—materials demands. *Appl Phys A*. 2001;72:619–623.
31. Chu XZ, Zhou YP, Su W, Sun Y, Zhou L. Adsorption of hydrogen isotopes on micro- and mesoporous adsorbents with orderly structure. *J Phys Chem B*. 2006;110(45):22596–22600.
32. Zhou L, Zhou YP, Sun Y. Studies on the mechanism and capacity of hydrogen uptake by physisorption-based materials. *Int J Hydrogen Energy*. 2006;31:259–264.
33. Wang K, Do DD. Characterizing the micropore size distribution of activated carbon using equilibrium data of many adsorbates at various temperatures. *Langmuir*. 1997;13:6226–6233.
34. Qiao SZ, Wang K, Hu XJ. Study of binary adsorption equilibrium of hydrocarbons in activated carbon using micropore size distribution. *Langmuir*. 2000;16:5130–5136.
35. Guo TM, et al. Multicomponent Vapor-Liquid Equilibrium and Distillation. Beijing: Chemical Engineering Press, 1983 (in Chinese).
36. Reich R, Ziegler WT, Rogers KA. Adsorption of methane, ethane, and ethane, and ethylene gases and their binary and ternary mixtures and carbon dioxide on activated carbon at 212–301K and pressures to 35 atmospheres. *Ind Eng Chem Process Des*. 1980;19:336–344.
37. Dreisbach F, Staudt R, Keller JU. High pressure adsorption data of methane, nitrogen, carbon dioxide and their binary and ternary mixtures on activated carbon adsorption. *Adsorption*. 1999;5:215–227.
38. Bai RS, Yang RT. A thermodynamically consistent langmuir model for mixed gas adsorption. *J Colloid Interface Sci*. 2001;239:296–302.

Appendix: Experimental Data

A. Adsorption equilibria of pure components

Table A1. Adsorption Data of H_2 on Activated Carbon JX101

T (K)							
283		298		313		328	
$10^{-6}p$ (Pa)	n (mmol g^{-1})	$10^{-6}p$ (Pa)	n (mmol g^{-1})	$10^{-6}p$ (Pa)	n (mmol g^{-1})	$10^{-6}p$ (Pa)	n (mmol g^{-1})
0.1700	0.0657	0.1470	0.0423	0.2260	0.0587	0.2360	0.0558
0.3430	0.1349	0.2985	0.0913	0.4210	0.1109	0.9245	0.2060
0.6585	0.2453	0.6135	0.1925	0.7285	0.1928	1.5795	0.3354
0.9625	0.3546	0.9255	0.2809	1.0190	0.2639	2.5180	0.4972
1.2785	0.4591	1.2285	0.3670	1.3245	0.3369	2.9845	0.5733
1.5825	0.5517	1.5285	0.4498	1.6525	0.4151		
1.9800	0.6714	1.9625	0.5645	2.0305	0.5007		
2.3540	0.7769	2.3580	0.6646	2.3845	0.5756		
2.7115	0.8809	2.6800	0.7397	2.7155	0.6413		
3.0770	0.9685	3.0435	0.8250	3.0815	0.7162		

Table A2. Adsorption Data of N_2 on Activated Carbon JX101

T (K)							
283		298		313		328	
$10^{-6}p$ (Pa)	n (mmol g^{-1})	$10^{-6}p$ (Pa)	n (mmol g^{-1})	$10^{-6}p$ (Pa)	n (mmol g^{-1})	$10^{-6}p$ (Pa)	n (mmol g^{-1})
0.3370	0.9962	0.2940	0.6892	0.3280	0.6032	0.2820	0.4133
0.5445	1.3942	0.5305	1.0898	0.5785	0.9480	0.4695	0.6507
0.7925	1.7817	0.8355	1.5062	0.8970	1.3041	0.8155	1.0042
1.1140	2.1712	1.1510	1.8509	1.2060	1.5956	1.1845	1.3323
1.4385	2.5017	1.4980	2.1607	1.5625	1.8711	1.5540	1.5839
1.7730	2.7779	1.8505	2.4206	1.9035	2.0896	1.8965	1.7981
2.1085	3.0153	2.1795	2.6353	2.2390	2.2893	2.2000	1.9612
2.4200	3.1938	2.5025	2.8149	2.5960	2.4727	2.4985	2.1093
2.7260	3.3523	2.8075	2.9706	3.0550	2.6697	2.7715	2.2383
3.0655	3.5047	3.1045	3.1053			3.1615	2.3929

Table A3. Adsorption Data of CH_4 on Activated Carbon JX101

T (K)							
283		298		313		328	
$10^{-6}p$ (Pa)	n (mmol g^{-1})	$10^{-6}p$ (Pa)	n (mmol g^{-1})	$10^{-6}p$ (Pa)	n (mmol g^{-1})	$10^{-6}p$ (Pa)	n (mmol g^{-1})
0.1001	1.1282	0.1656	1.3034	0.0641	0.4742	0.2805	1.1461
0.2625	2.2110	0.3235	1.9774	0.1507	0.9365	0.5245	1.7846
0.4910	3.0967	0.5295	2.6247	0.3675	1.7092	0.8575	2.4139
0.8395	3.9659	0.8490	3.3487	0.5880	2.3043	1.2125	2.9069
1.2135	4.5937	1.1970	3.9104	0.8950	2.9046	1.4865	3.2200
1.5160	4.9709	1.4745	4.2485	1.2270	3.3846	1.7690	3.5132
1.8985	5.3423	1.8555	4.6274	1.4810	3.7059	2.0345	3.7210
2.1845	5.5768	2.1510	4.8672	1.7380	3.9589	2.3370	3.9353
2.4900	5.7991	2.4450	5.0839	2.0130	4.1525	2.6705	4.1549
2.7895	5.9928	2.7755	5.2828	2.2795	4.3791	3.0180	4.3173
3.1270	6.1902	3.1330	5.4738	2.6040	4.5751		
				2.9385	4.7668		

Table A4. Adsorption Data of CO_2 on Activated Carbon JX101

T/K							
283		298		313		328	
$10^{-6}p$ (Pa)	n (mmol g^{-1})	$10^{-6}p$ (Pa)	n (mmol g^{-1})	$10^{-6}p$ (Pa)	n (mmol g^{-1})	$10^{-6}p$ (Pa)	n/mmol g^{-1}
0.0671	2.1960	0.0911	1.9747	0.0955	1.4690	0.1415	1.1803
0.1100	2.9425	0.1615	2.6696	0.1620	2.1183	0.2320	1.7850
0.2265	4.4859	0.2700	3.7056	0.3405	3.3797	0.4245	2.8381
0.4720	6.3302	0.5980	5.6195	0.5545	4.4940	0.7250	4.0045
0.8225	7.8983	0.8055	6.4113	0.8565	5.5436	1.0560	4.8497
1.1540	8.8295	1.0900	7.2142	1.2335	6.4827	1.3420	5.4103
1.4975	9.4985	1.4690	7.9769	1.5750	7.1192	1.6365	5.9224
1.8540	9.9371	1.9215	8.6133	1.9300	7.6161	1.9595	6.3722
2.1725	10.2250	2.3600	9.0487	2.1945	7.9119	2.2100	6.7137
2.5285	10.4332	2.6890	9.2846	2.4020	8.1117	2.4580	6.9277
2.8135	10.5322	3.0260	9.4783	2.5560	8.2897	2.7390	7.1780
3.1085	10.5861			2.8005	8.4513	3.0175	7.4206
				3.0115	8.6018		

B. Adsorption equilibria of mixtures

Table B1. Equilibrium Data Obtained for Run 1a

	Amount Adsorbed (mmol g^{-1})			
p/100 kPa	n (H_2)	n (N_2)	n (CH_4)	n (CO_2)
2.8738	4.0500E−02	1.8529E−01	5.1921E−01	1.6772
6.5176	7.1470E−02	3.1807E−01	8.8783E−01	2.5951
12.5069	1.1267E−01	4.3515E−01	1.2159E+00	3.5117
15.5186	1.3479E−01	4.7664E−01	1.3265E+00	3.8149
19.4654	1.6092E−01	5.2244E−01	1.4285E+00	4.2017
22.5558	1.8159E−01	5.4929E−01	1.4672E+00	4.3780
25.7153	2.0018E−01	5.6802E−01	1.5045E+00	4.5532

Table B2. Equilibrium Data Obtained for Run 1b

	Amount Adsorbed (mmol g^{-1})			
p/100 kPa	n (H_2)	n (N_2)	n (CH_4)	n (CO_2)
3.9062	4.3170E−02	1.9957E−01	5.0921E−01	1.2538
8.8014	8.1660E−02	3.1414E−01	9.1783E−01	2.2484
11.8627	1.0257E−01	3.7119E−01	1.0554E+00	2.6637
16.4623	1.2678E−01	4.3560E−01	1.2386E+00	3.0433
19.3233	1.4257E−01	4.7109E−01	1.3098E+00	3.3119
21.6970	1.5532E−01	5.0039E−01	1.3542E+00	3.4564
25.6230	1.7220E−01	5.3812E−01	1.4259E+00	3.6933

Table B3. Equilibrium Data Obtained for Run 1c

	Amount Adsorbed (mmol g^{-1})			
p/100 kPa	n (H_2)	n (N_2)	n (CH_4)	n (CO_2)
3.6119	3.8100E−02	1.6524E−01	4.1229E−01	0.9033
7.7541	6.8040E−02	2.6674E−01	6.9219E−01	1.6030
12.4690	1.0105E−01	3.4351E−01	9.1874E−01	2.0897
14.8143	1.1245E−01	3.7165E−01	1.0123E+00	2.3221
14.9622	1.1372E−01	3.7730E−01	1.0223E+00	2.3307
17.3584	1.2656E−01	4.0514E−01	1.1113E+00	2.4853
19.7880	1.3853E−01	4.3161E−01	1.1633E+00	2.6094
20.3657	1.4187E−01	4.3611E−01	1.1807E+00	2.6293
22.9717	1.5376E−01	4.5807E−01	1.2308E+00	2.7586
23.8632	1.5958E−01	4.6421E−01	1.2528E+00	2.7995
25.4483	1.6547E−01	4.7744E−01	1.2872E+00	2.9104
28.2018	1.7619E−01	4.9833E−01	1.3221E+00	3.0172

Table B4. Equilibrium Data Obtained for Run 1d

	Amount Adsorbed (mmol g^{-1})			
p/100 kPa	n (H_2)	n (N_2)	n (CH_4)	n (CO_2)
3.3409	4.0310E−02	1.4455E−01	3.0349E−01	0.5232
7.5376	7.2090E−02	2.3406E−01	5.7123E−01	1.0559
11.9367	9.4950E−02	3.0115E−01	7.8342E−01	1.3968
15.9019	1.1128E−01	3.5139E−01	9.5662E−01	1.7083
20.2349	1.2638E−01	3.9728E−01	1.0927E+00	1.9689
22.8031	1.3419E−01	4.2328E−01	1.1476E+00	2.1799
25.4212	1.4086E−01	4.4378E−01	1.2147E+00	2.2837
28.3169	1.5001E−01	4.6978E−01	1.2647E+00	2.4147

Table B5. Equilibrium Data Obtained for Run 2

	Amount Adsorbed (mmol g^{-1})			
p/100 kPa	n (H_2)	n (N_2)	n (CH_4)	n (CO_2)
3.1806	7.5520E−02	7.8190E−02	8.3039E−01	0.7021
7.0764	1.2821E−01	1.4225E−01	1.4063E+00	1.1803
10.5043	1.6584E−01	1.7840E−01	1.7858E+00	1.4932
15.3337	2.1254E−01	2.1878E−01	2.1206E+00	1.8735
19.0917	2.3787E−01	2.3957E−01	2.3068E+00	2.0702
23.3226	2.6589E−01	2.5888E−01	2.4854E+00	2.2680
26.4026	2.8451E−01	2.7145E−01	2.5757E+00	2.3634

Table B6. Equilibrium Data Obtained for Run 3

	Amount Adsorbed (mmol g^{-1})			
p/100 kPa	n (H_2)	n (N_2)	n (CH_4)	n (CO_2)
3.6370	6.7320E−02	2.0299E−01	4.8283E−01	0.6329
8.1962	1.1876E−01	3.4341E−01	9.1646E−01	1.1151
12.4870	1.6102E−01	4.3076E−01	1.2345E+00	1.4716
16.6339	1.9108E−01	5.0204E−01	1.4277E+00	1.6823
19.5979	2.0914E−01	5.4017E−01	1.5517E+00	1.8140
24.0147	2.3054E−01	5.8764E−01	1.6952E+00	1.9606
25.8240	2.3786E−01	6.0801E−01	1.7426E+00	1.9971

Table B7. Equilibrium Data Obtained for Run 4

	Amount Adsorbed (mmol g^{-1})			
p/100 kPa	n (H_2)	n (N_2)	n (CH_4)	n (CO_2)
1.7776	2.0540E−02	1.2501E−01	2.2655E−01	0.6837
4.2761	4.1860E−02	2.1910E−01	4.3309E−01	1.2095
7.1434	6.0880E−02	3.0976E−01	6.2501E−01	1.7234
7.7098	6.3550E−02	3.1975E−01	6.3941E−01	1.7740
11.0930	7.7020E−02	3.9816E−01	7.8214E−01	2.2084
14.7780	9.1610E−02	4.7319E−01	9.0889E−01	2.5911
18.3233	1.0077E−01	5.3155E−01	9.9622E−01	2.9245
18.3711	1.0179E−01	5.3217E−01	9.9657E−01	2.9364
26.1994	1.1967E−01	6.1321E−01	1.1383E+00	3.3976

Table B8. Equilibrium Data Obtained for Run 5

	Amount Adsorbed (mmol g^{-1})			
p/100 kPa	n (H_2)	n (N_2)	n (CH_4)	n (CO_2)
1.8087	2.5400E−02	9.3130E−02	1.9243E−01	0.3601
4.9696	5.5930E−02	1.7878E−01	4.0283E−01	0.7578
7.9923	7.6990E−02	2.4488E−01	5.8379E−01	1.1336
11.2094	9.3470E−02	3.0850E−01	7.4032E−01	1.4820
14.7135	1.0827E−01	3.5980E−01	8.6511E−01	1.7699
18.7493	1.2429E−01	4.1440E−01	9.8475E−01	2.0332
22.5484	1.3634E−01	4.6060E−01	1.0832E+00	2.2357
28.4768	1.5169E−01	5.1321E−01	1.2043E+00	2.5045

Manuscript received Jan. 8, 2007, and revision received Feb. 15, 2007.